arXiv:1201.0285v1 [cond-mat.str-el] 31 Dec 2011

# Magnetic Ordering in Carbon Nanotubes

Dmitri Yerchuck (a), Vyacheslav Stelmakh (a), Alla Dovlatova (b), Andrey Alexandrov (b), Yauhen Yerchak (a)
(a) - Belarusian State University, Nezavisimosti Avenue 4, Minsk, 220030,
RB (b) - M.V.Lomonosov Moscow State University, Moscow, 119899

(Dated: January 4, 2012)

The physical origin of the mechanism of the formation of ferromagnetic ordering in carbon nanotubes (NTs) produced by high energy ion beam modification of diamond single crystals in $\langle 110 \rangle$ and $\langle 111 \rangle$ directions has been found. It is determined by asymmetry of spin density distribution of Su-Schrieffer-Heeger topological soliton lattice formed in 1D Fermi quantum liquid state of $\pi$-electronic subsystem of given NTs. The phenomenon of formation of antiferromagnetic ordering coexisting with superconductivity at room temperature in carbon NTs, produced by high energy ion beam modification of diamond single crystals in $\langle 100 \rangle$ direction is discussed.

PACS numbers: 71.10.-w, 73.63.Fg, 78.30.-j, 76.30.-v, 76.50.+g, 78.67.-n
Keywords: magnetism, nanotubes, superconductivity

## I. INTRODUCTION AND BACKGROUND

It is well known that all substances on the whole are magnetics. At the same time, it is also well known, that classical magnetic ordering is existing in the substances, which are built from the atoms with unfilled inner atomic *d*- or *f*-shells or include given atoms in their elementary units. In other words, it is the substances, elementary units of which include transition chemical elements with unfilled atomic 3d-, 4d-, 5d-, 6d-shells, or 4f, 5f-shells of rare earth elements. Carbon does not refer to given group. Nevertheless, there are at present a number of communications on magnetic ordering in carbon and carbon based materials.

On the experimental revealing of magnetic ordering in carbon structurally ordered systems was reported for the first time during the IBMM-Conference in Knoxville, TN, USA [1] and it was confirmed in report on E-MRS Conference in Strasbourg, France [2]. Let us remark, that the first report almost in the same time on magnetic ordering in structurally non-ordered carbon materials is the work [3], where ferromagnetic ordering in pyrolytic carbon, produced by chemical vapour deposition (CVD) method using adamantane to be source material, was found. Let us also remark, that simultaneously, the reports [1], [2] were the first reports on the formation by high energy ion beam modification (HEIBM) of diamond single crystals structurally and magnetically ordered quasi-one-dimensional (quasi-1D) system along ion tracks, that is new carbon allotropic form, which was identified with nanotubes NTs, incorporated in diamond matrix in direction, precisely coinciding with ion beam direction. Given system possesses by a number of interesting physical properties, reported in [4], [7], [6]. When concerne the magnetic ordering, it was established from the study of temperature dependence of electron spin resonance (ESR) absorption intensity, that, for instance, incorporated nanotubes, produced by neon HEIBM of diamond single crystal along $\langle 100 \rangle$ crystallographic direction, possess by weak antiferromagnetic ordering [4], [7], [6]. At the same time, copper HEIBM with implantation direction along $\langle 111 \rangle$ crystal axis, nickel HEIBM with implantation direction along $\langle 110 \rangle$ axis [4], [7], [6] and boron HEIBM of polycrystalline diamond films with implantation direction transversely to film surface [5] lead to formation of NTs, incorporated in diamond matrix, which are possessed by ferromagnetic ordering. It was established directly by observation of ferromagnetic spin wave resonance (FMSWR) [5], [7], [6]. The first observations of FMSWR in carbon materials and in the materials, which are not traditional magnetic materials, on the whole, were reported in above cited works. It was established, that magnetic ordering is inherent property for carbon electronic system and it is not connected with magnetic impurities, since starting samples were selected in that way, that the absolute spin number of paramagnetic impurities and paramagnetic structural imperfections at all did not exceed the value $10^{12}$ spins. Very recently [9], antiferroelectric ordering has been found in the same pure carbon allotropic form - quasi-1D carbon zigzag-shaped nanotubes (CZSNTs), obtained by boron- and copper-HEIBM of diamond single crystals in $\langle 111 \rangle$-direction. It was established by means of the detection of new optical phenomenon - antiferroelectric spin wave resonance (AFESWR), which was theoretically described and experinmentally confirmed for the first time by infrared (IR) spectroscopy study of carbynes in [11]. It seems to be very new property of pure carbon allotropic forms - quasi-1D CZSNTs and carbynes. Moreover, on the observation of antiferroelectric ordering has been reported in [11] for the first time (to our knowlegde) for all matter systems on the whole. Given results mean, that pure carbon in the form of quasi-1D CZSNTs and carbynes is multiferroic system.

Let us remark, that experimental observation of multiferroicity in quasi-1D CZSNTs and carbynes means the breakdown of space inversion symmetry along CZSNT hypercomplex symmetry axis and carbyne chain symmetry axis. In the case of CZSNTs, it agrees well with the model of quasi-1D CZSNTs [8], [9], based on bond dimerization in all chain components of quasi-1D CZSNT along its hypercomplex symmetry axis $z$, which actually leads to inversion symmetry breakdown along given axis. Therefore, the experimental observation of antiferroelecricity of quasi-1D CZSNTs, necessary condition of which is the evident prediction of the model (appearance of nonzero polarisation by atomic displacements), proposed in [8], can be considered to be additional argument in favour of given model.

The aim of given work is to study in more details the properties of non-cylindrical nanotubes possessing instead $C_\infty$ symmetry axis the only $C_4$ symmetry axis and to establish the mechanisms of formation of magnetic and electric ordering in NTs both with $C_\infty$ symmetry axis and with $C_4$ symmetry axis, produced in diamond single crystals by high energy ion implantation.

## II. EXPERIMENTAL TECHNIQUE AND RESULTS

Samples of type IIa natural diamond, implanted by high energy ions of nickel (the energy of ions in ion beam was 335 $MeV$) have been studied. Paramagnetically pure samples have been selected so that the absolute spin number did not exceed the value $\approx 10^{12}$ spins in each of the sample used before implantation. Ion implantation was performed along $\langle 100 \rangle$ crystal direction (ion beam dose was $5 \times 10^{13}$ $cm^{-2}$), and in $\langle 110 \rangle$ crystal direction (ion beam dose was $5 \times 10^{14}$ $cm^{-2}$) transversely to sample (100) and (110) planes correspondingly uniformly along all the plane surface. The temperature of the samples during the implantation was controlled and it did not exceed 400 K. ESR spectra were registered on X-band ESR-spectrometer "Radiopan" at room temperature by using of $TE_{102}$ mode rectangular cavity. The ruby standard sample was permanently placed in the cavity on its sidewall. One of the lines of ESR absorption by $Cr^{3+}$ point paramagnetic centers (PC) was used for the correct relative intensity measurements of ESR absorption, for the calibration of the amplitude value of magnetic component of the microwave field and for precise phase tuning of microwave field. It was possible owing to unsaturating behavior of ESR absorption in ruby in the range of the microwave power applied, which was $\approx 100$ mW in the absence of attenuation. Unsaturable character of the absorption in a ruby standard was confirmed by means of the measurements of the absorption intensities in two identical ruby samples in dependence on the microwave power level. The first sample was standard sample, permanently placed in the cavity, the second sample was placed in the cavity so that the resonance line intensity was about 0.1 of the intensity of corresponding line of the first sample. They were registered simultaneously but their absorption lines were not overlapped owing to slightly different sample orientations. The foregoing intensity ratio was preserved for all microwave power values in the range used, which indicates, that really ruby samples are good standard samples in ESR spectroscopy studies.

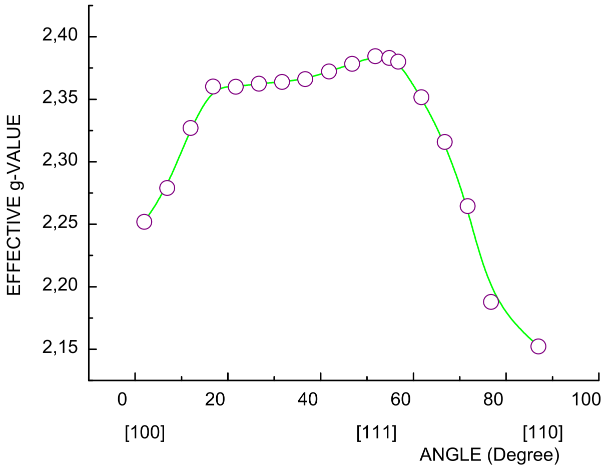

Figure 1: Angular dependence of effective g-value for the third FMSWR-mode, observed in NTs, incorporated in diamond single crystal by nickel ion beam direction transversely (110) sample plane

The studies of FMSWR in the sample implanted along $\langle 110 \rangle$ crystal direction were described in [7], however the mechanism of the ferromagnetically ordered state was not proposed. Let us summarise the results, which seems to be essential to establish the detailed processes, leading to ferromagnetism of incorporated carbon NTs, produced by $\langle 110 \rangle$ implantation. The strong anisotropy of spin wave excitation have been observed in unannealed samples. FMSWR was registered the only in the case, when the implantation plane was perpendicular to the vector $\vec{H}_1$ of magnetic component of the microwave field. The intensity of FMSWR absorption was increasing with temperature of isochronal 20-minutes annealing up to $\approx 700$ Celsius degrees. It is interesting, that after the annealing at 350 Celsius degrees and by higher temperatures FMSWR absorption was detected also by the vector $\vec{H}_1$ of magnetic component of the microwave field position, being to be parallel to sample implantation plane. The parameters of FMSWR absorption, that is splitting parameter, which can be characterised by, for instance, effective g-values of its modes, in particular by g-value of the third mode, Figure 1, and the modes' linewidths and intensities were strongly anisotropic. Angular dependencies of the linewidth, FMSWR absorption amplitude and intensity of the third FMSWR-mode are presented in Figures 2 to 4.

The splitting parameter anisotropy seems to be nontrivial, it characterises by two maxima - at 54.7 degrees, that is, in [111] direction of diamond lattice, and in direction about 17 degrees from [100] crystal direction. It is interesting, that unlike to $\langle 111 \rangle$ ion beam modification [4], the angular dependence of linewidth has the resemblance with the angular dependence of g-value, it characterises also by two maxima at the same angles,

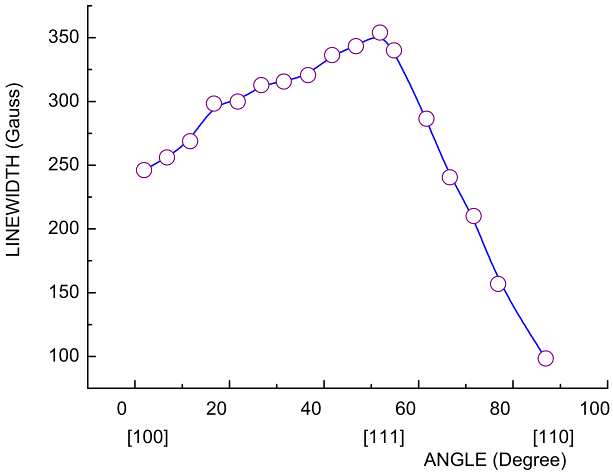

Figure 2: Angular dependence of the linewidth of the third FMSWR-mode, observed in NTs, incorporated in diamond single crystal by nickel ion beam direction transversely (110) sample plane

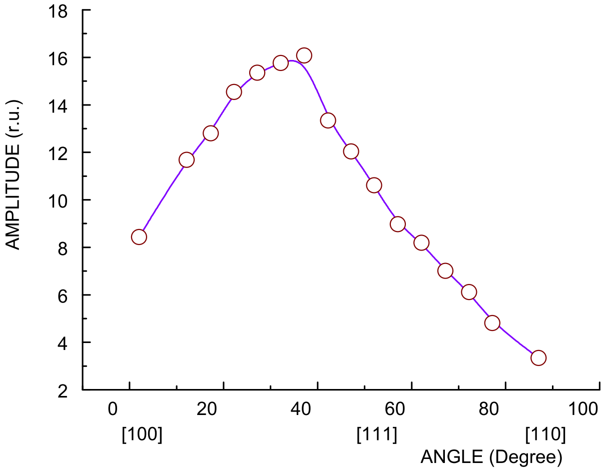

Figure 3: Angular dependence of FMSWR absorption amplitude of the the third FMSWR-mode, observed in NTs, incorporated in diamond single crystal by nickel ion beam direction transversely (110) sample plane

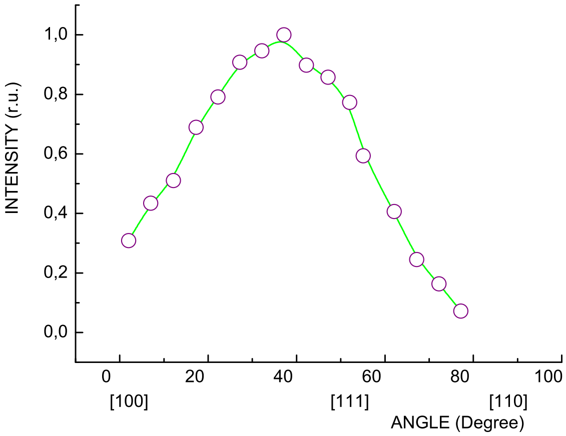

Figure 4: Angular dependence of the FMSWR absorption intensity of the third FMSWR-mode, observed in NTs, incorporated in diamond single crystal by nickel ion beam direction transversely (110) sample plane

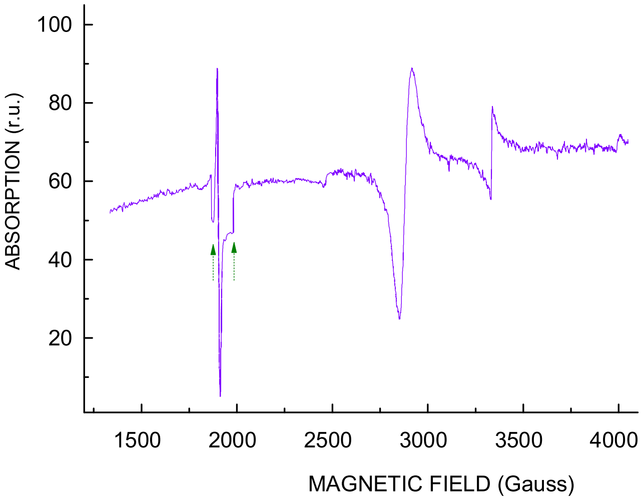

Figure 5: Spectral distribution of ESR absorption intensity in diamond single crystal, implanted by high energy nickel ions by beam direction transversely (100) sample plane, the sample was rotated in $(0\bar{1}1)$ plane, $\vec{H}_0 ||$ [100] crystal axis

see Figure 2. (At ⟨111⟩ ion beam modification minimum of g-value, for instance, for main FMSWR-mode corresponds to maximum of linewidth value). Minimal effective g-value and minimal value of linewidth for the third mode are achieved at [110] direction and they are equal to 2.1526 and to 100 G respectively, maximal effective g-value and maximal value of linewidth correspond to [111] direction of diamond lattice and are equal respectively to 2.3845 and 360 G. Coinciding of the directions of anisotropy maxima with diamond lattice characteristic directions is indication of the role of host diamond lattice on the characteristics of magnetic ordering. It is also strong evidence, that magnetic ordering is determined by electron-electron correlations in valence $\pi$-subsystem of electronic system (but not in $\sigma$-subsystem), since the only $\pi$-subsystem can be subjected to so strong response on the surrounding lattice presence by NT formation, which is starting at more lower ion fluences, and strong response seems to be preserved by entire HEIBM of near surface region in diamond single crystal. Amplitude dependence, Figure3, is characterised by one clearly pronounced maximum near 35.3 degrees direction of diamond lattice, that is, it coincides also with symmetry

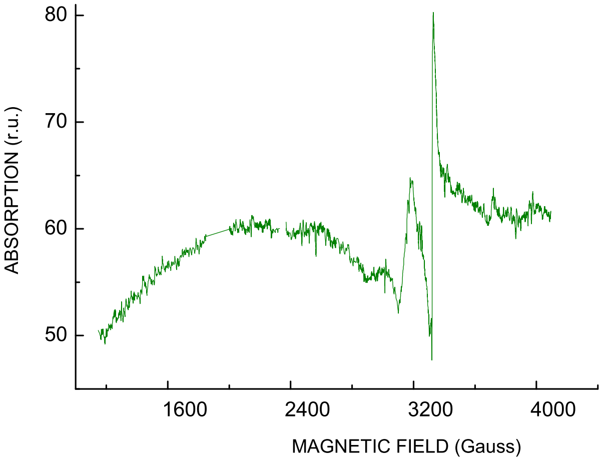

Figure 6: Spectral distribution of ESR absorption intensity in diamond single crystal, implanted by high energy nickel ions by beam direction transversely (100) sample plane, the sample was rotated in $(0\overline{1}1)$ plane, $\vec{H}_0||$ [111] crystal axis

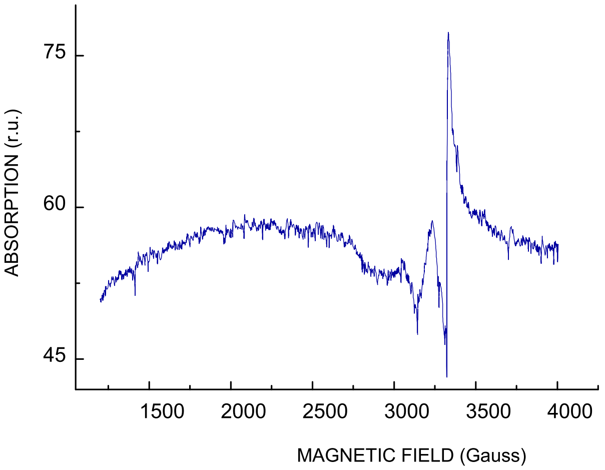

Figure 7: Spectral distribution of ESR absorption intensity in diamond single crystal, implanted by high energy nickel ions by beam direction transversely (100) sample plane, the sample was rotated in $(0\overline{1}1)$ plane, the angle between $\vec{H}_0$ and [100] crystal axis is 60 degrees

direction of diamond lattice. It is seen, that amplitude dependence is also strongly anisotropic. So, amplitude change is equal to 4.8 times. It is additional indication that mechanism of magnetic ordering is connected with the formation of ordered structures just in $\pi$-subsystem of incorporated NTs. Simultaneously, it is the display of the fact, that anisotropy of FMSWR absorption by magnetically ordered NT-structure and the anisotropy of magnetically ordered NT-structure itself are different.

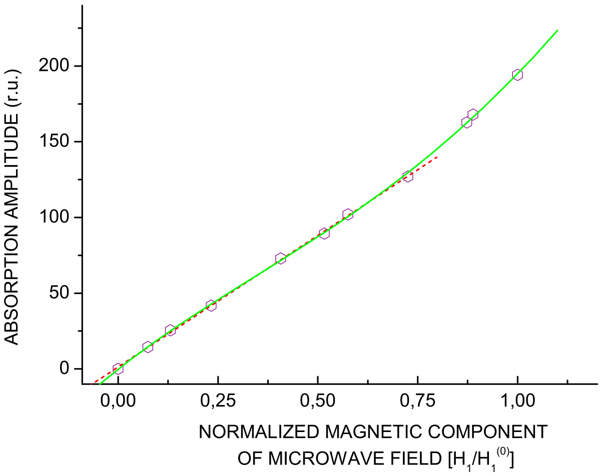

Figure 8: Dependence of absorption amplitude of the left line in ESR spectrum of NTs incorporated in diamond single crystal on magnetic component of microwave field at $\vec{H}_0||$ [100] crystal axis

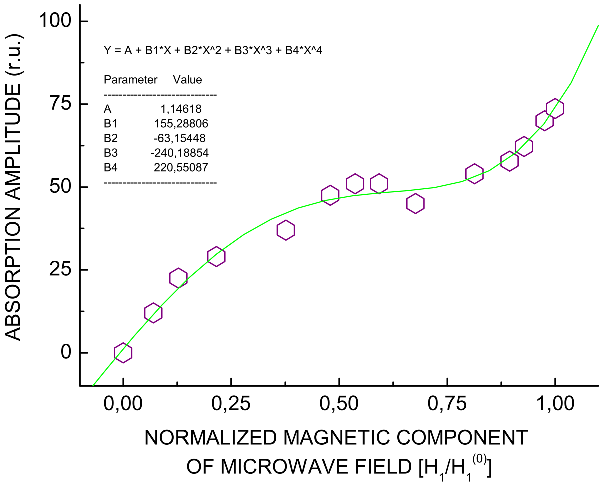

Figure 9: Dependence of absorption amplitude of the right broad line in ESR spectrum of NTs incorporated in diamond single crystal on magnetic component of microwave field at $\vec{H}_0||$ [100] crystal axis

Two not very pronounced maxima at 54.7 degrees and in direction near 17 degrees from [100] crystal are appeared additionally to the maximum near 35.3 degrees direction in the angular dependence of the intensity, Figure 4. They are determined by contribution of linewidth anisotropy, compare Figure 4 and Figure 2.

The ESR spectra observed in carbon nanotubes (NTs), produced by nickel high energy $\langle 100 \rangle$ ion beam modification of natural diamond single crystals, are presented in Figures 5 to 7 in crystal directions [100], [111] and 60 degrees from [100] correspondingly. The line in the range (1865 - 1981) G (it is indicated by arrows in Figure 4) is the absorption line by ruby standard, it isshifted to botton in Figure 5 and it is removed in the same range in Figure 6. The most intensive lines, belonging to the sample studied, were excited spontaneously the only by very precise orientation of external static magnetic field $\vec{H}_0$ in the direction coinciding with implantation direction and resulting spectrum was consisting of three lines, at that two lines have rather large anisotropic linewidths. Let us designate given lines by $R_b$ for the right broad line and by L for the left line. The right broad line was overlapped with relatively narrow almost isotropic line, designated by $R_n$ (given line was observed by usual sample orientation). Additionally, very broad strongly intensive anisotropic absorption with two dip positions at $\sim 2410$ G and $\sim 2892$ G in the direction corresponding [111] diamond lattice direction, Figure 6, is detected, which are overlapped by static magnetic field direction in 60 degrees from [100] diamond crystal direction, Figure 7. It seems to be the display of the fact, that the symmetry of the interaction, leading to the appearance of very strong absorption is determined by inherent symmetry of NTs, produced by [100] HEIBM, which is not connected with potential effect of diamond lattice presence.

Dependence of absorption amplitude of L-line and $R_b$ line on magnetic component of microwave field at fixed orientation of polarising magnetic field $\vec{H}_0||$ [100] crystal axis have been studied, Figures 8 and 9. It is seen from comparison of the Figures 8 and 9, that given dependencies are quite different. The dependence, presented for L-line in Figure 8 is superlinear. It is similar to the dependencies, which were earlier observed in the samples, modified by HEIBM with copper, neon, nickel ions (however with dose $5\times10^{14}$) [4], [7], [6], that is, in the case of entire near surface layer modification. In the studied sample (integral dose is $5\times10^{13}$), individual NTs are isolated by diamond structure, nevertheless the superlinear dependence is taking place, which seems to be unexpected. Let us remark, that the initial part of the curve, presented in Figure 8, can in the principle be approximated by a linear dependence (dashed line), although it is clear from comparison with the approximation of the whole curve, solid line in Figure 8, that even initial part, strongly speaking, is not linear. Solid line in Figure 8 is the polinomial fit with the function $f(x) = b_0 + b_1x + b_2x^2 + b_3x^3 + b_4x^4$, where $b_0 = -0.17117$, $b_1 = 208.92305$, $b_2 = -139.06624$, $b_3 = 159.14424$, $b_4 = -33.90983$.

Dependence of absorption amplitude of the right broad line $R_b$ in ESR spectrum of NTs on magnetic component of microwave field is strongly nonlinear. It is characterised for the values of relative magnetic component of microwave field $H_1/H_1^{(0)}$ in the range (0-0.75) by usual saturating law, but in the range (0.75-1) it acquires prominent superlinear nonsaturating character. The dependence for ESR absorption kinetics in the form of presented in Figure 9 is observed in ESR-spectroscopy for

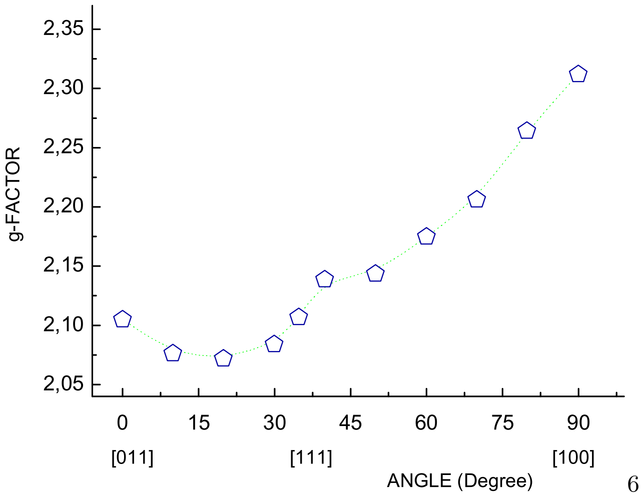

Figure 10: Angular dependence of g-factor of the left line in ESR spectrum of NTs incorporated in diamond single crystal, the sample was rotated in $(0\overline{1}1)$ plane

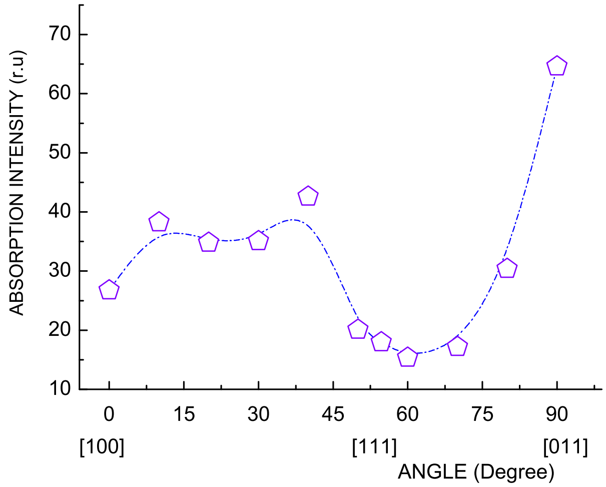

Figure 11: Angular dependence of ESR absorption intensity of the left line in ESR spectrum of NTs incorporated in diamond single crystal, the sample was rotated in $(0\overline{1}1)$ plane

the first time. It can be approximated by the solid line, which represents itself the polynomial fit in accordance with relation $Y(x) = A + B_1x + B_2x^2 + B_3x^3 + B_4x^4$, where $A = 1.14618$, $B_1 = 0.77956$, $B_2 = -0.00159$, $B_3 = -3.03868E-5$, $B_4 = 1.40072E-7$. Angular dependence of g-factor of the left line L in ESR spectrum of NTs in the sample studied is presented in Figure 10. It consist of two branches. One branch is in the angle range 0-60 degrees from [100] crystal lattice direction (which is coinciding with NT axis direction), the second branch is in the angle range 60-90 degrees. Let us remark that the connection point of two branches, equaled to 60 degrees for the g-values of L-line is coinciding with

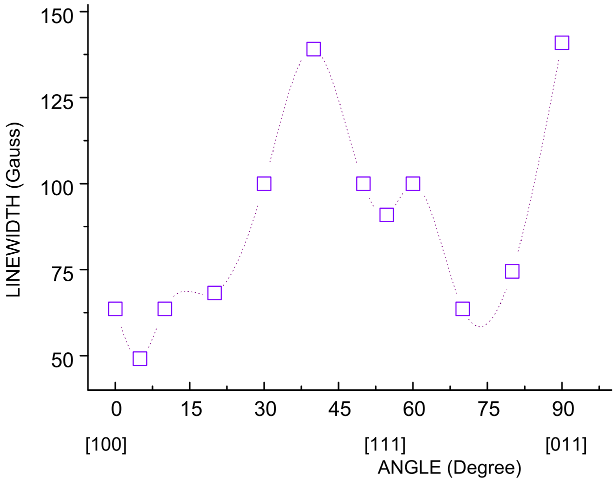

Figure 12: Angular dependence of linewidth of the left line in ESR spectrum of NTs incorporated in diamond single crystal, the sample was rotated in $(0\bar{1}1)$ plane

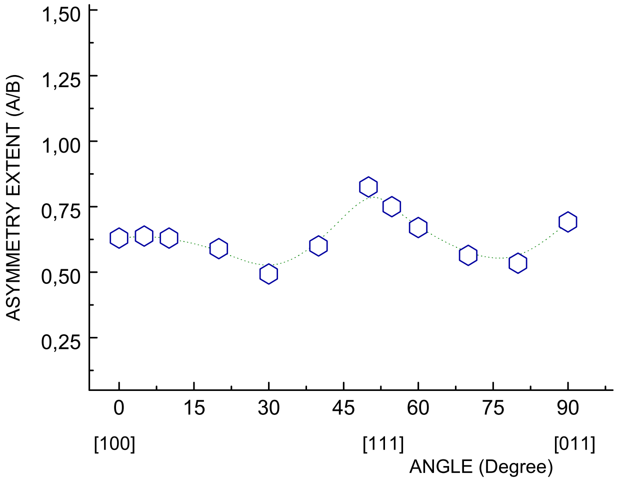

Figure 13: Angular dependence of asymmetry extent A/B of the left line in ESR spectrum of NTs incorporated in diamond single crystal, the sample was rotated in $(0\bar{1}1)$ plane

the point of the junction of two dips in the very broad (and consequently very intensive) absorption, testifying on the same or related nature of the resonance processes, which are responsible for the appearance of L-line and very broad lines. The deviation of g-values from free electron value g = 2.0023 is very large, at that the minimal value is achieved in the range 16-20 degrees from the [011] direction in diamond lattice and it is equal to ≈ 2.0719, maximal g-value corresponds to NT axis direction, that is to [100] crystal lattice direction and it is equal to ≈ 2.3120. Given values are characteristic for the systems with the strong magnetic ordering. Consequently, we have obtained the direct proof of the spontaneous transition of NT system, incorporated in diamond lattice, in the state with the strong magnetic ordering. Angular dependence of ESR absorption intensity of the left line L has qualitatively opposite character. The maximal absorption value corresponds to the direction, being to be transversal to NT axis, which is coincides with [011] direction in diamond lattice, Figure 11. Additional maximum is observed at 60 degrees from given direction. Let us remark that both the maxima in angular dependence of ESR absorption intensity of the line L are observed also in angular dependence of linewidth, Figure 12, indicating that the main features in given dependence are governed by angular dependence of linewidth. It is confirmed also by that, the very pronounced maximum in the angular dependence of absorption amplitude of line L is in the range 10-20 degrees from [100] crystal lattice direction (the corresponding Figure is not presented). At the same time it is not pronounced in angular dependence of absorption intensity, see Figure 11. Especially interesting, that the line L is asymmetric, Figure 13. However numerical values of the ratio A/B of the asymmetry extent are quite different in comparison with those ones by usual Dyson shape [24]. The value A/B is equal 2.55 for static (immobile) PC in conductive media and it is determined by by the space dispersion contribution [25], which is appeared in conductive media. It corresponds to the space dispersion contribution and absorption contribution to resulting ESR response equal to (1 : 1) [25]. The value A/B for absorption derivative is increasing from 2.55 to more than 19 for mobile PC in dependence on velocity of the spin diffusion [26]. It is seen from Figure 13 that the ratio A/B is less than 1 and it is strongly

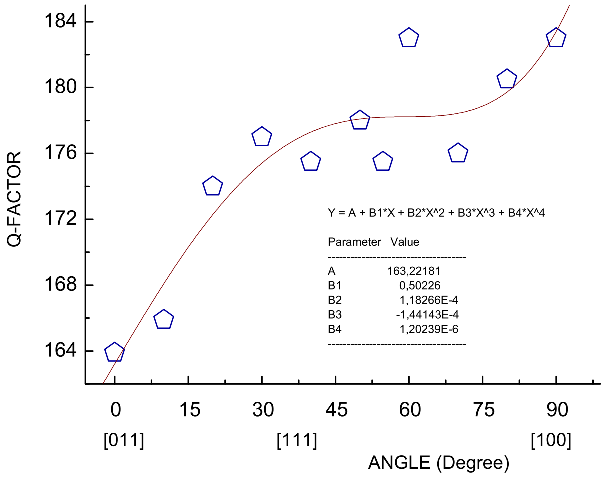

1

Figure 14: Angular dependence of the cavity Q-factor with the sample implanted by high energy nickel ions by beam direction transversely (100) sample plane, the sample was rotated in $(0\bar{1}1)$ plane

anisotropic. The maximal A/B value is near [111] crystal lattice direction and it is equal to 0.83, Figure 13. The minimal A/B value is near 30 degree from [100] crystal lattice direction and it is equal to 0.49, Figure 13. The presence of the ruby standard has allowed to control the cavity Q-factor, Figure 14. It seems to be substantial that Q-factor is increasing in the range where A/B value is decreasing, that is near 30 degrees and in the range near 70-80 degrees, compare Figure 14 and Figure 13.

## III. DISCUSSION

Although it was established, that copper HEIBM with implantation direction along $\langle 111\rangle$ crystal axis, nickel HEIBM with implantation direction along $\langle 110\rangle$ axis, and boron HEIBM of polycrystalline diamond films with implantation direction transversely to film surface lead to formation of NTs, incorporated in diamond matrix, which possess by ferromagnetic orderingn [4], [7], [6], [5] the nature of given state and mechanism, leading to its formation was not theoretically described. To solve given task, it seems to be necessary to know the nature of charge and spin carriers and the mechanisms of carrier transport and interactions of charge and spin carriers both between themselves and with phonons and photons. There seems to be paramount significant the same task for nanoelectronics, spintronics and for the other branches of nanotechnology. There is existing in the theory of 1D electronic systems in particular in the theory of conducting NTs the following concept, which was starting with the work of Tomonaga in 1950 [16] and with the work by Luttinger in 1963 [17], when it has become clear that the electron-electron interaction destroys the sharp Fermi surface and leads to a breakdown of the Landau Fermi liquid (LFL) theory. The resulting non-LFL state is commonly called Luttinger liquid (LL), or sometimes Tomonaga-Luttinger liquid to describe the universal low-energy properties of 1D conductors. LL behavior is characterized by pronounced power-law suppression of the transport current and the density of states, and by effect of spin-charge separation. The nature of the spin and charge carriers was also established. They are chargeless spin 1/2 quasiparticles - spinons and spinless quasiparticles with the charge ± e - holons. The universality of LL description means that the physical properties do not depend on details of the model, the interaction potential, and so on, but instead are only characterized by a few parameters - critical exponents. Quite remarkably, the LL concept is believed to hold for arbitrary statistical properties of the particles, that is both for fermions and bosons. It provided a paradigm for non-Fermi liquid physics. It is argued in many works, that the single-wall carbon nanotubes (SWCNTs), considered to be 1D objects (it is not always correct, especially for standard NTs with diameter in several nanometers) can be described the only in the frame of LL concept. Moreover, SWCNTs are considered to be the best model system of the LL state demonstration. Really, power-law behavior was observed experimentally by measuring the tunneling conductance of SWNTs in dependence on temperature and voltage. Electron force microscopic measurements showed also the ballistic nature of transport in conducting SWNTs. At the same time spin-charge separation has not been observed so far. Therefore, the existing viewpoint seems to be insufficiently grounded.

It has to be remarked, that both the models LL and LFL are the models of ideal (and even oversimplified) quantum liquids, since they do not take into account the nonlinearity of the fermion spectrum on the one hand and electron-phonon interactions on the other hand. In fact both the models describe not strongly adequately the real processes, since the changes in charge state of arbitrary atom in 1D chain to be the result of electron-electron interaction are always accompanied by the changes in phonon subsystem (and vice versa). It is consequence of generic coupling between operators of creation and annihilation in electron subsystem and in phonon field. Let us also remember, that key argument for insertion of the notion "Luttinger liquid" is in fact the simplification, determined by linearization of the generic spectrum of particles in neighborhood of Fermi points in k-space. Just given simplification has led to divergencies arising in the perturbation theory in 1D-case and it does not means that 1D Fermi liquid description is incorrect in general case. Consequently, the description of NTs the only in the frames of LL concept seems to be also oversimplification. Moreover, it is showed in [10] that the concept of description of 1D correlated electronic systems in the frame of 1D Fermi liquid (FL) can be renewed. The most interesting it was found, that the Fermi liquid concept can be applied just to 1D carbon NTs, while 2D NTs and graphene can be in principle described in the low energy physics processes in the frame of LL model. It was considered in [10] the concept of 1D FL on the example of well known 1D system - *trans*-polyacetylene (t-PL), that is, it is in fact the generalization of well known Fermi gas SSH-model [15], [15], which, however, in distinction from LFL and LL models, takes into account the electron-phonon interaction. The subsequent generalization, for instance, for application of given model immediately to quasi-1D carbon zigzag shaped nanotubes can be easily obtained by using of hypercomplex number theory like to the works [8], [9], where hypercomplex number theory was applied for the interpretation of quantum optics effects in NTs.

Let us summarise briefly for the convenience of the readers the results, presented in [10].

The Born-Oppenheimer approximation was considered and starting Hamiltonian is the following

$$\hat{\mathcal{H}}(u) = \hat{\mathcal{H}}_0(u) + \hat{\mathcal{H}}_{\pi,t}(u) + \hat{\mathcal{H}}_{\pi,u}(u). \tag{1}$$

The first term in (1) is

$$\hat{\mathcal{H}}_0(u) = \sum_m \sum_s \left(\frac{\hat{P}_m^2}{2M^*}\hat{a}^+_{m,s}\hat{a}_{m,s} + K u_m^2 \hat{a}^+_{m,s}\hat{a}_{m,s}\right). \tag{2}$$

It represents itself the sum of operator of kinetic energy of CH-group motion (the first term in (2)) and the operator of the $\sigma$-bonding energy (the second term). Coefficient $K$ in (2) is effective $\sigma$-bonds spring constant, $M^*$ is total mass of CH-group, $u_m$ is configuration coordinate for $m$-th CH-group, which corresponds to translation of $m$-th CH-group along the symmetry axis $z$ of the chain, $m = \overline{1,N}$, $N$ is number of CH-groups in the chain, $\hat{P}_m$ is operator of impulse, conjugated to configuration coordinate $u_m$, $m = \overline{1,N}$, $\hat{a}^+_{m,s}$, $\hat{a}_{m,s}$ are creation and annihilation operators of creation or annihilation of quasiparticle with spin projection $s$ on the $m$-th chain site in $\sigma$-subsystem of t-PA. The second term in (1) can be represented in the form of two components and it is

$$\begin{aligned}&\hat{\mathcal{H}}_{\pi,t}(u) = \hat{\mathcal{H}}_{\pi,t_0}(u) + \hat{\mathcal{H}}_{\pi,t,\alpha_1}(u) = \\ &\sum_m\sum_s[(t_0(\hat{c}^+_{m+1,s}\hat{c}_{m,s} + \hat{c}^+_{m,s}\hat{c}_{m+1,s})] + \\ &(-1)^m 2\alpha_1 u)(\hat{c}^+_{m+1,s}\hat{c}_{m,s} + \hat{c}^+_{m,s}\hat{c}_{m+1,s})],\end{aligned} \tag{3}$$

where $\hat{c}^+_{m,s}$, $\hat{c}_{m,s}$ are creation and annihilation operators of creation or annihilation of quasiparticle with spin projection $s$ on the $m$-th chain site in $\pi$-subsystem of t-PA. It is the resonance interaction (hopping interaction in tight-binding model approximation) of quasiparticles in $\pi$-subsystem of t-PA electronic system, which is considered to be Fermi liquid, and in which the only constant and linear terms in Taylor series expansion of resonance integral about the dimerized state are taking into account.

Operator $\hat{\mathcal{H}}(u)$ is invariant under spatial translations with period $2a$, where $a$ is projection of spacing between two adjacent CH-groups in undimerized lattice on chain axis direction, and which is equal to 1.22 $\mathring{A}$. It means, that all various wave vectors $\vec{k}$ in $\vec{k}$-space will be in reduced zone with module of $\vec{k}$ in the range $-\frac{\pi}{2a} \leq k \leq \frac{\pi}{2a}$ [15]. It can be considered like to usual semiconductors to be consisting of two subzones - conduction ($c$) band and valence ($v$) band. Then it seems to be convenient to represent the operators $\{\hat{c}^+_{m,s}\}$, $\{\hat{c}_{m,s}\}$, $m = \overline{1,N}$, in the form

$$\begin{aligned}\{\hat{c}_{m,s}\} &= \{\hat{c}^{(c)}_{m,s}\} + \{\hat{c}^{(v)}_{m,s}\}, \\ \{\hat{c}^+_{m,s}\} &= \{\hat{c}^{+(c)}_{m,s}\} + \{\hat{c}^{+(v)}_{m,s}\},\end{aligned} \tag{4}$$

related to $\pi - c$- and $\pi - v$-band correspondingly, and to define $\vec{k}$-space operators

$$\begin{aligned}\{\hat{c}^{(c)}_{k,s}\} &= \{\frac{i}{\sqrt{N}}\sum_m\sum_s(-1)^{m+1}\exp(-ikma)\hat{c}^{(c)}_{m,s}\}, \\ \{\hat{c}^{(v)}_{k,s}\} &= \{\frac{1}{\sqrt{N}}\sum_m\sum_s\exp(-ikma)\hat{c}^{(v)}_{m,s}\},\end{aligned} \tag{5}$$

$m = \overline{1,N}$.

The $\sigma$-operators $\{\hat{a}^+_{m,s}\}$ and $\{\hat{a}_{m,s}\}$, $m = \overline{1,N}$ can also be represented in the form like to (4) for $\pi$-operators and analogous to (5), transforms can be defined. Then the expression for the operator $\hat{\mathcal{H}}_0(u)$ can be rewritten

$$\begin{aligned}&\hat{\mathcal{H}}_0(u) = \hat{\mathcal{H}}^{\sigma,c}_0(u) + \hat{\mathcal{H}}^{\sigma,v}_0(u) = \sum_m\sum_s(\frac{\hat{P}^2_m}{2M^*} + Ku^2_m)\times \\ &\frac{1}{N}\sum_k(\hat{a}^{+\sigma,c}_{k,s}\hat{a}^{\sigma,c}_{k,s} + \hat{a}^{+\sigma,v}_{k,s}\hat{a}^{\sigma,v}_{k,s}),\end{aligned} \tag{6}$$

where $\hat{a}^{+\sigma,c}_{k,s}$, $\hat{a}^{\sigma,c}_{k,s}$ and $\hat{a}^{+\sigma,v}_{k,s}$, $\hat{a}^{\sigma,v}_{k,s}$ are $\sigma$-operators of creation and annihilation, related to $\sigma$-$c$-band and to $\sigma$-$v$-band correspondingly. The independence of $|u_m|$ on $m$, $m = \overline{1,N}$, means, that the expression $(\frac{\hat{P}^2_m}{2M^*} + Ku^2_m)$ is independent on $m$. Then we obtain

$$\hat{\mathcal{H}}_0(u) = \sum_k\sum_s(\frac{\hat{P}^2}{2M^*} + Ku^2)(\hat{n}^{\sigma,c}_{k,s} + \hat{n}^{\sigma,v}_{k,s}), \tag{7}$$

where $\hat{n}^{\sigma,c}_{k,s}$ and $\hat{n}^{\sigma,v}_{k,s}$ are operators of number of $\sigma$-quasiparticles in $\sigma$-$c$-band and $\sigma$-$v$-band correspondingly.

The expression for $\hat{\mathcal{H}}_{\pi,t_0}(u)$ in terms of $\{\hat{c}^{(c)}_{k,s}\}$ and $\{\hat{c}^{(v)}_{k,s}\}$ is coinciding with known corresponding expression in [14], [15] and it is

$$\hat{\mathcal{H}}_{\pi,t_0}(u) = \sum_k\sum_s 2t_0\cos ka(\hat{c}^{+(c)}_{k,s}\hat{c}^{(c)}_{k,s} - \hat{c}^{+(v)}_{k,s}\hat{c}^{(v)}_{k,s}) \tag{8}$$

The expression for the second part of operator $\hat{\mathcal{H}}_{\pi,t}(u)$ in terms of $\{\hat{c}^{(c)}_{k,s}\}$ and $\{\hat{c}^{(v)}_{k,s}\}$ is also coinciding in its form with known corresponding expression in [14], [15] and it is given by

$$\hat{\mathcal{H}}_{\pi,t,\alpha_1}(u) = \sum_k\sum_s 4\alpha_1 u\sin ka(\hat{c}^{+(v)}_{k,s}\hat{c}^{(c)}_{k,s} + \hat{c}^{+(c)}_{k,s}\hat{c}^{(v)}_{k,s}), \tag{9}$$

where subscript $\alpha_1$ in Hamiltonian designation indicates on the taking into account the part of electron-phonon interaction, connected with resonance interaction (hopping) processes. The expression for the operator $\hat{\mathcal{H}}_{\pi,u}(u)$, which describes the part of electron-phonon interaction, determined by interaction between quasiparticles in Fermi liquid state of $\pi$-subsystem in terms of $\{\hat{c}^{(c)}_{k,s}\}$ and $\{\hat{c}^{(v)}_{k,s}\}$ is the following

$$\hat{\mathcal{H}}_{\pi,u,\alpha_2}(u) = \sum_k\sum_{k'}\sum_s \alpha_2(k,k',s)\hat{c}^{+(c)}_{k',s}\hat{c}^{+(v)}_{k',s}\hat{c}^{(v)}_{k,s}\hat{c}^{(c)}_{k,s}. \tag{10}$$

Here the consideration is restricted by the taking into account the contribution of the term, corresponding to interaction between the quasiparticles in different bands, which seems to be the most essential. Physically the identification of linear on displacement $u$ part of both resonance interaction (hopping) and the pairwise interaction of quasiparticles in $\pi$-subsystem between themselves with electron-phonon interaction is understandable, if to take into account, that by atomic $CH$ group displacements the phonons are generated, which in its turn can by release of the place on, for instance, $(CH)_m$ group, to deliver the energy and impulse, which are necessary for transfer of the quasiparticle (electron) from adjacent $(m-1)$- or $(m+1)$-position in chain in the case of resonance interaction (hopping). For the case the pairwise interaction of quasiparticles, it means, that its linear on displacement $u$ part is realized by means of phonon field, which transfers the energy and impulse from one quasiparticle to another (which can be not inevitable adjacent). Mathematically it can be proved in the following way. The processes of interaction in $c$ $(v)$ band can be considered to be independent on each other. It means, that transition probability from the $\langle k_{l,s}|$-state to $\langle k_{j,s}|$-state in $c$-band and from $\langle k'_{l,s}|$-state to $\langle k'_{j,s}|$-state in $v$-band, which is proportional to coefficient $\alpha_2(k,k',s)$, can be expressed in the form of product of real parts of corresponding matrix elements, that is in the form

$$\begin{aligned}&\alpha_2(k,k',s) \sim Re\langle k_{l,s}|\hat{V}^{(c)}|k_{j,s}\rangle Re\langle k'_{l,s}|\hat{V}^{(v)}|k'_{j,s}\rangle = \\ &\sum_{k_{ph}} Re\langle k_{l,s}|\hat{V}^{(c)}|k_{ph}\rangle\langle k_{ph}|k_{j,s}\rangle\times \\ &\sum_{k_{ph}} Re\langle k'_{r,s}|\hat{V}^{(v)}|k_{ph}\rangle\langle k_{ph}|k'_{n,s}\rangle,\end{aligned} \tag{11}$$

where $\hat{V}^{(v)} = V_{0(v)}\hat{e}$ ($\hat{e}$ is unit operator) is the first term in Taylor expansion of pairwise interaction of quasiparticles, for instance, with wave vectors $k'_r$, $k'_n$ and spin projection $s$ in $v$-band, that is, in ground state, $\hat{V}^{(c)} = V_{1(c)}u\hat{e}$ is the second term in Taylor expansion of pairwise interaction in excited state (in c-band), that is, it is product of configuration coordinate $u$ and coordinate derivative at $u = 0$ of operator of pairwise interaction of quasiparticles with wave vectors $k_l$, $k_j$ and spin projection $s$ in $c$-band, $k_{ph}$ is phonon wave vector, and the summation is realized over all the phonon spectrum. At that, since the linear density of pairwise interaction is independent on $k$, which is the consequence of translation invariance of the chain, $V_{0(v)}$, $V_{1(c)}$ are constants. Therefore, the pairwise interaction is considered to be accompanying by process of phonon generation, when electronic quasiparticles are already in excited state, that is, in $c$-band (retardation effect of phonon subsystem is taken into account). Then we have $\hat{V}^{(c)} = V_{0(c)}u\hat{e}$, $\hat{V}^{(v)} = V_{0(v)}\hat{e}$. A number of variants are possible along with process of phonon generation, corresponding to states of electronic quasiparticles in $c$-band above described. The result will mathematically be quite similar, if to change the energetic place of excitation, that is, if to interchange the role of $c$ and $v$ bands for given process. There seem to be possible the realization of both the stages (that is phonon generation and absorption) for electronic quasiparticles in single $c$ or $v$ band states and simultaneous realisation both the stages in both the bands. Mathematical description will be for all possible variants similar and for distinctness, it was considered only the first variant. For the simplicity, the processes were considered, in which the spin projection is keeping to be the same. It is evident also, that in $z$-direction the impulse distribution is quasi-continuous (since the chain has the macroscopic length $L = Na$). Consequently, standard way $\sum_{k_{ph}} \rightarrow \frac{L}{2\pi}\int_{k_{ph}}$ can be used. Further, phonon states can be described by wave functions $\langle k_{ph}| = v_0 exp(ik_{ph}z)$, where $z \in [0,L]$, $k_{ph} \in [-\frac{\pi}{2a}, \frac{\pi}{2a}]$, $v_0$ is constant. Therefore, it is obtained from (11) the expression

$$\begin{aligned}&\alpha_2(k,k',s) = b|v_{0v}|^2|v_{0c}|^2 V_{0(c)}uV_{0(v)}|\phi_{0cs}|^2|\phi_{0vs}|^2\times \\ &\frac{N}{2\pi(q_l-q_j)(q_r-q_n)} Re\{\exp[i(k_l m_l - k_j m_j)a]\exp ika\}\times \\ &Re\{\exp[i(k'_r m_r - k'_n m_n)a]\exp ik'a\},\end{aligned} \tag{12}$$

where $|\phi_{0cs}|^2$, $|\phi_{0vs}|^2$ are squares of the modules of the wave functions $|k_{j,s}\rangle$ and $|k'_{j,s}\rangle$ respectively, $k = k_{ph}(q_l - q_j)$, $k' = k'_{ph}(q_r - q_n)$ $q_l, q_j, q_r, q_n \in N$ with additional conditions $(q_l - q_j)a \le L$, $(q_r - q_n)a \le L$, $b$ - is aspect ratio, which in principle can be determined by comparison with experiment. Here the values $(q_l - q_j)$, $(q_r - q_n)$ determine the steps in pairwise interaction with phonon participation and they are considered to be fixed. We will consider The processes, for which $k = k'$, are considered. Consequently, $(q_r - q_n) = (q_l - q_j)$ and the operator $\hat{\mathcal{H}}_{\pi,u,\alpha_2}(u)$ is

$$\begin{aligned}&\hat{\mathcal{H}}_{\pi,u,\alpha_2}(u) = \\ &\sum_k\sum_{k'}\sum_s 4\alpha_2 u \sin ka \sin k'a\hat{c}^{+(c)}_{k',s}\hat{c}^{+(v)}_{k',s}\hat{c}^{(v)}_{k,s}\hat{c}^{(c)}_{k,s},\end{aligned} \tag{13}$$

where $4\alpha_2(s)$ is

$$\begin{aligned}&b|v_{0v}|^2|v_{0c}|^2 V_{0(c)}V_{0(v)}|\phi_{0cs}|^2|\phi_{0vs}|^2\times \\ &\frac{N}{2\pi[(q_l-q_j)]^2} = 4\alpha_2(s)\end{aligned} \tag{14}$$

The system of operators $\hat{c}^{+(c)}_{k',s}$, $\hat{c}^{+(v)}_{k',s}$, $\hat{c}^{(v)}_{k,s}$, $\hat{c}^{(c)}_{k,s}$ corresponds to noninteracting quasiparticles, and it is understandable, that in the case of interacting quasiparticles their linear combination has to be used

$$\begin{bmatrix}\hat{a}^{(v)}_{k,s}\\ \hat{a}^{(c)}_{k,s}\end{bmatrix} = \begin{bmatrix}\alpha_{k,s} & -\beta_{k,s}\\ \beta_{k,s} & \alpha_{k,s}\end{bmatrix}\begin{bmatrix}\hat{c}^{(v)}_{k,s}\\ \hat{c}^{(c)}_{k,s}\end{bmatrix}, \tag{15}$$

Then the Hamiltonian $\hat{\mathcal{H}}_{\pi,t,\alpha_1}(u)$, which corresponds to SSH one-electron treatment of electron-phonon coupling, can be represented in the form

$$\begin{aligned}&\hat{\mathcal{H}}_{\pi,u,\alpha_1}(u) = \\ &\sum_k\sum_s \Delta_k[\alpha^2_{k,s}\hat{a}^{+(v)}_{k,s}\hat{a}^{(c)}_{k,s} - \alpha_{k,s}\beta_{k,s}\hat{a}^{+(v)}_{k,s}\hat{a}^{(v)}_{k,s} \\ &+ \beta_{k,s}\alpha_{k,s}\hat{a}^{+(c)}_{k,s}\hat{a}^{(c)}_{k,s} - \beta^2_{k,s}\hat{a}^{+(c)}_{k,s}\hat{a}^{(v)}_{k,s} + \alpha^2_{k,s}\hat{a}^{+(c)}_{k,s}\hat{a}^{(v)}_{k,s} \\ &+ \alpha_{k,s}\beta_{k,s}\hat{a}^{+(c)}_{k,s}\hat{a}^{(c)}_{k,s} - \beta_{k,s}\alpha_{k,s}\hat{a}^{+(v)}_{k,s}\hat{a}^{(v)}_{k,s} - \beta^2_{k,s}\hat{a}^{+(v)}_{k,s}\hat{a}^{(c)}_{k,s}],\end{aligned} \tag{16}$$

where $\Delta_k = 4\alpha_1 u \sin ka$. The diagonal part $\hat{\mathcal{H}}^d_{\pi,t,\alpha_1}(u)$ of operator $\hat{\mathcal{H}}_{\pi,u,\alpha_1}(u)$ is

$$\hat{\mathcal{H}}^d_{\pi,t,\alpha_1}(u) = \sum_k \sum_s 2\Delta_k \alpha_{k,s}\beta_{k,s}(\hat{n}^{(c)}_{k,s} - \hat{n}^{(v)}_{k,s}), \tag{17}$$

where $\hat{n}^{(c)}_{k,s}$ is density of operator of quasiparticles' number in $c$-band, $\hat{n}^{(v)}_{k,s}$ is density of operator of quasiparticles' number in $v$-band. The part of pairwise interaction, which is linear in displacement coordinate $u$ and leads to participation of the phonons, is given by the Hamiltonian

$$\begin{aligned}
&\hat{\mathcal{H}}_{\pi,u,\alpha_2}(u) = \sum_k \sum_{k'} \sum_s 4\alpha_2 u \sin ka \sin k'a \times \\
&(\alpha^2_{k',s}\hat{a}^{+(c)}_{k',s}\hat{a}^{(v)}_{k',s} - \beta^2_{k',s}\hat{a}^{(v)}_{k',s}\hat{a}^{+(c)}_{k',s} \\
&+ \alpha_{k',s}\beta_{k',s}\hat{a}^{(c)}_{k',s}\hat{a}^{+(c)}_{k',s} - \beta_{k',s}\alpha_{k',s}\hat{a}^{(v)}_{k',s}\hat{a}^{+(v)}_{k',s}) \\
&\times (\alpha^2_{k,s}\hat{a}^{+(c)}_{k,s}\hat{a}^{(v)}_{k,s} - \beta^2_{k,s}\hat{a}^{+(v)}_{k,s}\hat{a}^{(c)}_{k,s} \\
&+ \alpha_{k,s}\beta_{k,s}\hat{a}^{+(c)}_{k,s}\hat{a}^{(c)}_{k,s} - \beta_{k,s}\alpha_{k,s}\hat{a}^{+(v)}_{k,s}\hat{a}^{(v)}_{k,s}).
\end{aligned} \tag{18}$$

The diagonal part $\hat{\mathcal{H}}^d_{\pi,u,\alpha_2}(u)$ of operator $\hat{\mathcal{H}}_{\pi,u,\alpha_2}(u)$ is

$$\begin{aligned}
&\hat{\mathcal{H}}^d_{\pi,u,\alpha_2}(u) = 4\alpha_2 u \sum_k \sum_{k'} \sum_s \alpha_{k'}\beta_{k'}(\hat{n}^{(v)}_{k',s} - \hat{n}^{(c)}_{k',s}) \\
&\times \alpha_{k,s}\beta_{k,s}(\hat{n}^{(v)}_{k,s} - \hat{n}^{(c)}_{k,s}) \sin k'a \sin ka
\end{aligned} \tag{19}$$

Let us remark, that the Hamiltonian $\hat{\mathcal{H}}_{\pi,u,\alpha_2}(u)$ describes the attraction between the electrons, it can lead to formation of Cooper pairs in a $\pi$-subsystem and to superconductivity.

The Hamiltonian $\hat{\mathcal{H}}_{\pi,t}(u)$ in terms of operator variables $\hat{a}^{(c)}_{k,s}$ $\hat{a}^{(v)}_{k,s}$ is

$$\begin{aligned}
&\hat{\mathcal{H}}_{\pi,t}(u) = \sum_k \sum_s 2t_0 \cos ka[(\alpha^2_{k,s} - \beta^2_{k,s})(\hat{a}^{+(c)}_{k,s}\hat{a}^{(c)}_{k,s} - \\
&\hat{a}^{+(v)}_{k,s}\hat{a}^{(v)}_{k,s}) - 2\alpha_{k,s}\beta_{k,s}(\hat{a}^{+(v)}_{k,s}\hat{a}^{(c)}_{k,s} + \hat{a}^{+(c)}_{k,s}\hat{a}^{(v)}_{k,s})]
\end{aligned} \tag{20}$$

The diagonal part $\hat{\mathcal{H}}^d_{\pi,t_0}(u)$ of operator $\hat{\mathcal{H}}_{\pi,t_0}(u)$ is given by the relation

$$\hat{\mathcal{H}}^d_{\pi,t_0}(u) = \sum_k \sum_s \epsilon_k(\alpha^2_{k,s} - \beta^2_{k,s})(\hat{n}^{(c)}_{k,s} - \hat{n}^{(v)}_{k,s}), \tag{21}$$

where $\epsilon_k = 2t_0 \cos ka$.

The operator transformation for the $\sigma$-subsystem, analogous to (15) shows, that the Hamiltonian $\hat{\mathcal{H}}_0(u)$ is invariant under given transformation, that is, it can be represented in the form, given by (7).

To find the values of elements of matrix in relation 15), the Hamiltonian $\hat{\mathcal{H}}(u)$ has been tested for conditional extremum in dependence on the variables $\alpha_k$, $\beta_k$ with condition $\alpha^2_{k,s} + \beta^2_{k,s} = 1$.

Two values for the energy of quasiparticles, indicating on the possibility of formation of the quasiparticles of two kinds both in $c$-band and $v$-band have been obtained. They are the following

$$\begin{aligned}
E^{(c)}_k(u) &= \frac{\mathcal{Q}^2\Delta^2_k - \epsilon^2_k}{\sqrt{\epsilon^2_k + \mathcal{Q}^2\Delta^2_k}}, \\
E^{(v)}_k(u) &= \frac{\epsilon^2_k - \mathcal{Q}^2\Delta^2_k}{\sqrt{\epsilon^2_k + \mathcal{Q}^2\Delta^2_k}}
\end{aligned} \tag{22}$$

and

$$\begin{aligned}
E^{(c)}_k(u) &= \sqrt{\epsilon^2_k + \mathcal{Q}^2\Delta^2_k}, \\
E^{(v)}_k(u) &= -\sqrt{\epsilon^2_k + \mathcal{Q}^2\Delta^2_k}
\end{aligned} \tag{23}$$

The factor $\mathcal{Q}$ is determined by relation

$$[1 + \frac{\alpha_2}{2\alpha_1} \sum_k \sum_s \frac{\mathcal{Q}\Delta_k \sin ka}{\sqrt{\epsilon^2_k + \mathcal{Q}^2\Delta^2_k}}(n^{(c)}_{k,s} - n^{(v)}_{k,s})] = \mathcal{Q}, \tag{24}$$

where $n^{(c)}_{k,s}$ is eigenvalue of density operator of quasiparticles' number in $c$-band, $n^{(v)}_{k,s}$ is eigenvalue of density operator of quasiparticles' number in $v$-band. The quasiparticles with the energy, determined by (23) at $\mathcal{Q} = 1$ are the same quasiparticles, that were obtained in known SSH-model.

Sufficient conditions for the minimum of the functions $E(\alpha_{k,s}\beta_{k,s})$ can be obtained by standard way, which was used in [9]. It consist in that, that the second differential of the energy being to be the function of three variables $\alpha_{k,s}$, $\beta_{k,s}$ and $\lambda_{k,s}$ has to be positively defined quadratic form. From the condition of positiveness of three principal minors of quadratic form coefficients the three sufficient conditions for the energy minimum have been obtained. Their analysis has showed, that SSH-like solution is inapplicable for the description of standard processes, passing near equilibrium state by any parameters. The quasiparticles, described by SSH-like solution, can be created the only in strongly nonequilibrium state with inverse population of the levels in $c$- and $v$-bands. At the same time the solution, the energy of quasiparticles for which is determined by (22) can be realised both in near equilibrium and in strongly non-equilibrium states of the $\pi$-subsystem of t-PA, which is considered to be quantum Fermi liquid.

The continuum limit for the ground state energy of the $t$-PA chain with SSH-like quasiparticles will coincide with known solution [15], if to replace $\Delta_k\mathcal{Q} \rightarrow \Delta_k$. The calculation of the ground state energy $E^{[u]}_0(u)$ of the $t$-PA chain with quasiparticles' branch, which is stable near equilibrium by taking into account, that in ground state $n^c_{k,s} = 0$, $n^v_{k,s} = 1$, in the continuum limit gives

$$E^{[u]}_0(u) = -\frac{2Na}{\pi} \int\limits_0^{\frac{\pi}{2a}} \frac{(\mathcal{Q}\Delta_k)^2 - \epsilon^2_k}{\sqrt{\mathcal{Q}\Delta_k)^2 + \epsilon^2_k}} dk + 2NKu^2. \tag{25}$$

Then, calculation of the integral results in the expression

$$E_0^{[u]}(u) = \frac{4Nt_0}{\pi}\{F(\frac{\pi}{2}, 1-z^2)+ \\ \frac{1+z^2}{1-z^2}[E(\frac{\pi}{2}, 1-z^2) - F(\frac{\pi}{2}, 1-z^2)]\} + 2NKu^2, \tag{26}$$

where $z^2 = \frac{2\mathcal{Q}\alpha_1 u}{t_0}$, $F(\frac{\pi}{2}, 1-z^2)$ is the complete elliptic integral of the first kind and $E(\frac{\pi}{2}, 1-z^2)$ is the complete elliptic integral of the second kind. Approximation of ground state energy at $z \ll 1$ for the stable near equilibrium solution gives

$$E_0^{[u]}(u) = N\{\frac{4t_0}{\pi} - \frac{6}{\pi}\ln\frac{2t_0}{\mathcal{Q}\alpha_1 u}\frac{4(\mathcal{Q}\alpha_1)^2u^2}{t_0}+ \\ \frac{28(\mathcal{Q}\alpha_1)^2u^2}{\pi t_0} + ...\} + 2NKu^2. \tag{27}$$

It is seen from (27), that the energy of quasiparticles, described by given solution, has the form of Coleman-Weinberg potential with two minima at the values of dimerization coordinate $u_0$ and $-u_0$ like to the energy of quasiparticles, described by SSH-solution. It is understandable, that subsequent considerations, including electrically neutral S=1/2 soliton and electrically charged spinless soliton formation, that is the appearance of the phenomenon of spin-charge separation, by FL description of 1D systems will be coinciding in its mathematical form with those ones in Fermi gas SSH-model.

Thus, the possibility to describe the physical properties of 1D systems in the frames of 1D quantum FL including the mechanism of appearance of the most prominent feature of 1D systems - the phenomenon of spin-charge separation - is proved.

So, the model proposed takes into consideration the electron-electron correlations in explicit form, which seems to be ground for its application to electronic system of quasi-1D NTs, where electron-electron correlations are known to be rather strong. In particular, it can be used for analysis of ESR and FMSWR spectra. It can be done by above indicated manner, that is by using of hypercomplex number theory analogously to theoretical analysis of quantum optics effects in [8] and analysis in [9] of Raman spectra in quasi-1D NTs. It seems to be also substantial, that FL treatment of electron-phonon interaction extends the applicability limits of SSH-model of 1D conjugated conductors allowing its use in the case of strong electron-phonon interaction and (or) strong electron-photon interaction. It is evident, that the mechanism of the phenomenon of spin-charge separation in 1D FL is topological soliton mechanism, which is quite different from Anderson spinon-holon mechanism. Anderson mechanism of spin-charge separation is realised in fact for the systems with the linear function of the electronic energy in dependence on quasi-wave vector $\vec{k}$ for rather large energy interval. Just 2D NTs and graphene possess by given peculiarity, although the corresponding energy interval is relatively narrow.

The results obtained show, that the shape of $\pi$-solitons (or $\sigma$-solitons) is given by the expression with the same mathematical form both in Fermi gas SSH-model and in its FL consideration. It is

$$|\phi(n)|^2 = \frac{1}{\xi_{\pi(\sigma)}}sech^2[\frac{(n-n_0)a}{\xi_{\pi(\sigma)}} - v_{\pi(\sigma)}t]\cos^2\frac{n\pi}{2}, \tag{28}$$

where $n, n_0$ are variable and fixed numbers of $CH$-unit in $CH$-chain, $a$ is $C-C$ interatomic spacing projection on chain direction, $v_{\pi(\sigma)}$ is $\pi$ ($\sigma$)-soliton velocity, $t$ is time, $\xi_{\pi(\sigma)}$ is $\pi(\sigma)$ coherence length. It is seen, that $\pi$-solitons ($\sigma$-solitons) differ in fact by numerical value of coherence length in Fermi gas SSH-model and in its FL description. Really, the coherence length $\xi_\pi$ and $\xi_{0\sigma}$ is determined by the relation [22]

$$\xi_{0\pi} = \frac{\hbar v_F}{\Delta_{0\pi}}, \xi_{0\sigma} = \frac{\hbar v_F}{\Delta_{0\sigma}}, \tag{29}$$

where $\Delta_{0\sigma}$, $\Delta_{0\pi}$ are $\sigma-$ and $\pi$-bandgap values at $T = 0K$, $v_F$ is Fermi velocity. In SSH Fermi gas model $v_F$ is proportional to $t_0$, in SSH FL-model, here presented, $v_F$ is proportional to sum $t_0 + t_1$. It allows to explain some discrepancy between theoretical value in Fermi gas model and experimental values for $\xi_\pi$ and its dispersion, depending on production technology. Theoretical value in Fermi gas model for $\xi_\pi$ in t-PA is $7a$, and it is low boundary in the range $7a - 11a$, obtained for $\xi_\pi$ from experiments [18]. It means, that in the samples with $\pi$-soliton coherence length, equaled to $11a$ $t_1$ is equal to $0.57t_0$ at the same t-PA band gap value (it is possible, since factor $\mathcal{Q}$ is independent on $t_1$ and can be close to 1). It means, that constant component $t_1$ in Taylor expansion of electron-electron interaction potential is substantial and that it depends on preparation technology.

The observation of FMSWR phenomenon in the NTs, formed by $\langle 110\rangle$ high energy nickel ion implantation in natural diamond single crystal (at ion beam dose in $5 \times 10^{14}$ $cm^{-2}$) unambiguously means, that the SSH $\pi$-soliton lattice formation takes place, that is periodical non-harmonic spin-density wave. For the simplicity we can approximate the function of the shape of given density wave (let us designate it with abbreviation ASLSDW (Approximation of Soliton Lattice Spin Density Wave) by trapeziform function, Fig.14. Real function of the envelope shape of soliton lattice spin density wave will be between given trapeziform function and harmonic sinusoidal function for density wave HSDW (Harmonic Spin Density Wave). We will show, that given approximation is rather good for qualitative and in the principle for quantitative estimation of characteristics of ferromagnetic order formation. Actually, from mathematical viewpoint the difference between these states is minimal since ASLSDW can be represented in the form of superposition of HSDWs, where amplitude of main harmonic is strongly exceeding the others. It follows from the expansion of ASLSDW profile in Fourier series, which is

$$f(x') = A(2L_0 + L_1)\sum_{m=0}^{\infty}\left\{\frac{\left[2(2L_0+L_1)\left(\cos\frac{\pi m L_0}{2L_0+L_1} - \cos\frac{\pi m(L_0+L_1)}{2L_0+L_1}\right) - \pi L_1 m \sin m\pi\right]}{2L_1\pi^2 m^2}\cdot\cos\frac{2\pi m x'}{L}\right\}, \tag{30}$$

$$f(x) = A(2L_0 + L_1)\left[\frac{1}{4} + (2L_0+L_1)\sum_{m=1}^{\infty}\frac{\left(\cos\frac{\pi m L_0}{2L_0+L_1} - \cos\frac{\pi m(L_0+L_1)}{2L_0+L_1}\right)}{2L_1\pi^2 m^2}\cdot\cos\frac{2\pi m x}{L}\right]. \tag{31}$$

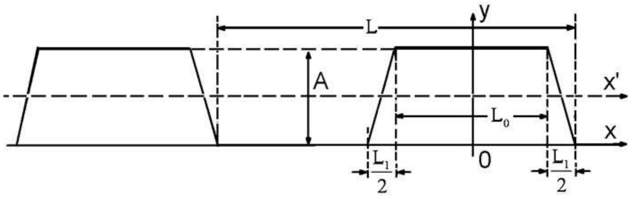

Figure 15: Approximation of soliton lattice spin (charge) density wave profile along the chain direction

The sense of the parameters $L_0$, $L_1$, L is seen from Fig.15. The functions $f(x)$, $f(x')$ denote spin density distributions $S(x)$, $S(x')$ in the case of ASLSDW and charge density distributions $\rho(x)$, $\rho(x')$ in the case of ASLCDW. Expression (30) corresponds to position of chain atoms along $X'$-direction, Fig.15. Expression (31) corresponds to position of chain atoms along $X$-direction, Fig.15. We see, that by asymmetric deviation of spin (or charge) density relatively the chain direction, the constant component is appeared. It will lead in the case of real SLSDW to ferromagnetic ordering if density wave distribution is magnetic spin density wave distribution and to ferroelectric ordering by similar electric dipole density distribution. One can also see from (30) and (31), that the amplitude of components with m $> 1$ is inversely proportional to $m^2$, that is, it diminishes rather quickly when number $m$ increases. In the first order approximation, the relations (30) and (31) can be represented by

$$f(x') = A\,(2L_0 + L_1)\,\alpha\cos\frac{2\pi x'}{L} + o\left(\frac{1}{m^2}\right), \tag{32}$$

$$f(x) = A\,(2L_0 + L_1)\left(\frac{1}{4} + \frac{1}{2}\alpha\cos\frac{2\pi x}{L}\right) + o\left(\frac{1}{m^2}\right), \tag{33}$$

where $\alpha$ is

$$\alpha = \frac{\left[(2L_0+L_1)\left(\cos\frac{\pi L_0}{2L_0+L_1} - \cos\frac{\pi(L_0+L_1)}{2L_0+L_1}\right)\right]}{L_1\pi^2}. \tag{34}$$

It is seen from (28), that envelope function of single soliton spin density distribution corresponds precisely to the case with $x$ axis position, that is, it is strongly asymmetric relatively the chain axis. By the formation of the soliton lattice the periodic envelope function of soliton spin density distribution in soliton lattice will be determined by overlapping of individual envelope functions and the asymmetry extent can be even more pronounced depending on overlapping extent. Let us also remark, that given conclusion is preserved, when simultaneously with Peierls metal-insulator transition the Mott-Hubbard metal-insulator transition also takes place, it leads to modification of oscillating factor in (28). Instead of factor $\cos^2\frac{n\pi}{2}$ the factor $(b_1\cos^2\frac{n\pi}{2} - b_2\sin^2\frac{n\pi}{2})$ is appeared, at that in real case of t-PA $b_1$ is substantially exceeds $b_2$, although it is nonzero [23]. Further, it was found also, that there is numerical coincidence of the characteristics of SSH topological $\pi$-solitons in t-PA and in quasi-1D CZSNTS, formed both by $\langle 111\rangle$ and $\langle 110\rangle$ ion implantation. So, the values of g-tensor components in $Cu$-implanted sample are $g_1 = 2.00255$ (it is minimal $g$-value and it is $g_{||}$ principal direction), $g_2 = g_3 = g_\perp = 2.00273$, the accuracy of relative g-value measurements is $\pm 0.00002$ [4]. $g$-value of paramagnetic $\pi$-solitons in t-PA, equaled to 2.00263 [19], gets in the middle of given rather narrow interval of $g$-value variation of PC in ion produced NTs. Although anisotropy of paramagnetic $\pi$-solitons in $t$-PA, mapping the distribution of $\pi$-electron density along the whole individual $t$-PA chain, is not resolved by ESR measurements directly, there are indirect evidences on axial symmetry of ESR absorption spectra in $t$-PA too, [20], [21]. Consequently, the value 2.00263 is mean value and it coincides with accuracy 0.00002 with average value of aforecited principal $g$-tensor values of PC in quasi-1D CZSNTs. Taking into account given high precision coincidence of g-values in t-PA and quasi-1D CZSNTs we can conclude that SSH-$\pi$-soliton density distribution in quasi-1D CZSNTs is also asymmetric along hypercomplex $x$-axis. Then, the appearance of ferromagnetic ordering in quasi-1D CZSNTs, formed by $\langle 111\rangle$ and $\langle 110\rangle$ ion implantation is explained by a natural way.

Therefore we have found the physical origin of the mechanism of the formation of ferromagnetic ordering in carbon NTs. It determines the only by $\pi$-subsystem of full electronic system, which agrees well with experimental results on FMSWR above summarised and explains qualitatively the sensitivity of FMSWR parameters, presented in Figures 1 to 4 to symmetry directions of surrounding diamond crystal lattice by $\langle 110\rangle$ implantation.

Experimental results obtained by ESR study of NTs, formed in diamond single crystals in the result of the $\langle 100\rangle$ ion beam modification indicates, that for the correct description of Nts' properties the $\sigma$-electronic subsystem has to be taken into consideration. It follows immediately from the appearance of inherent symmetry directions in distinction to $\langle 110\rangle$ ion beam modification, whre ferromagnetic ordering symmetry characteristics are governed by symmetry directions of surrounding diamond lattice.

Let us consider the following Hamiltonian

$$\hat{\mathcal{H}}(u) = \hat{\mathcal{H}}_0(u) + \hat{\mathcal{H}}_1(u) + \hat{\mathcal{H}}_2(u) + \hat{\mathcal{H}}_3(u) + \hat{\mathcal{H}}_4(u), \quad (35)$$

where $u$ is configuration coordinate, which corresponds to translation of CH-groups along the symmetry axis $z$ of the chain, it is suggested to be independent on site position and on subsystem kind. Operator $\hat{\mathcal{H}}_0(u)$ is

$$\hat{\mathcal{H}}_0(u) = \sum_{\vec{k}} \sum_m \sum_q \sum_s \varepsilon^{mq}(u) \hat{c}^+_{\vec{k}ms} \hat{c}_{\vec{k}qs}, \quad (36)$$

in which subscripts $m, q = \{\pi, \sigma\}$, $s$ is spin projection, $\vec{k}$ is wave vector, $\hat{c}^+_{\vec{k}ms}$, $\hat{c}_{\vec{k}ms}$ are operators of creation and annihilation of the quasiparticle with spin projection $s$ and wave vector $\vec{k}$ in $m$th ($q$th) subsystem, $\varepsilon^{mq}(u)$ are the resonance interaction integrals (hopping interaction in tight-binding model approximation) of quasiparticles in $\pi$-subsystem of t-PA electronic system, in $\sigma$-subsystem of t-PA electronic system which are considered to be Fermi liquids, and between $\pi$- and $\sigma$-subsystems.

$\hat{\mathcal{H}}_1$ is

$$\hat{\mathcal{H}}_1(u) = \sum_m \sum_j U_1(j, m, u) \hat{c}^+_{jms(\uparrow)} \hat{c}_{jms(\uparrow)} \hat{c}^+_{jms(\downarrow)} \hat{c}_{jms(\downarrow)}, \quad (37)$$

where $j = \overline{1, N}$ is the site position $U_1(j, m, u)$ is intrasubsystem Coulomb coupling parameter, which is dependent in general case on $j, m, u$. The operator $\hat{\mathcal{H}}_2(u)$ is

$$\hat{\mathcal{H}}_2(u) = \sum_{m>q} \sum_j U_2(j, m, q, u) \sum_s \hat{c}^+_{jms} \hat{c}_{jms} \sum_s \hat{c}^+_{jqs} \hat{c}_{jqs} \quad (38)$$

where $U_2(j, m, q, u)$ is intersubsystem Coulomb coupling parameter, which is dependent in general case on $j, m, q, u$. The operator $\hat{\mathcal{H}}_3(u)$ is

$$\hat{\mathcal{H}}_3(u) = \sum_{m>q} \sum_j \sum_s \sum_{s'} J_1(j, m, q, u) \hat{c}^+_{jms} \hat{c}^+_{jqs'} \hat{c}_{jms'} \hat{c}_{jqs}, \quad (39)$$

where $J_1(j, m, q, u)$ is the inter-subsystem Hund's rule coupling, which is dependent in general case on $j, m, q, u$. The operator $\hat{\mathcal{H}}_4(u)$ is

$$\hat{\mathcal{H}}_4 = \sum_{m \neq q} \sum_j J_2(j, m, q, u) \hat{c}^+_{jms(\uparrow)} \hat{c}^+_{jms(\downarrow)} \hat{c}_{jqs(\downarrow)} \hat{c}_{jqs(\uparrow)} \quad (40)$$

where $J_2(j, m, q, u)$ is pair hopping parameter, which is dependent in general case on $j, m, q, u$.

Like to foregoing consideration the Hamiltonians $\hat{\mathcal{H}}_1(u)$ and $\hat{\mathcal{H}}_2(u)$ can be expanded in Taylor series about the dimerized state. So, we have

$$\begin{aligned} \hat{\mathcal{H}}_1(u) = \sum_m \sum_j (U_1^{(0)} + \\ (-1)^j 2\alpha_1^m u) \hat{c}^+_{jms(\uparrow)} \hat{c}_{jms(\uparrow)} \hat{c}^+_{jms(\downarrow)} \hat{c}_{jms(\downarrow)}, \end{aligned} \quad (41)$$

where $\{\alpha_1^m\}$, $m = \{\pi, \sigma\}$ are constants of electron-phonon interactions, accompanying the processes of intrasubsystem Coulomb interations.

$$\begin{aligned} \hat{\mathcal{H}}_2(u) = \sum_{m>q} \sum_j (U_2^{(0)} + \\ (-1)^j 2\alpha_2^{mq} u) \sum_s \hat{c}^+_{jms} \hat{c}_{jms} \sum_s \hat{c}^+_{jqs} \hat{c}_{jqs}, \end{aligned} \quad (42)$$

where $\{\alpha_2^{mq}\}$, $m, q = \{\pi, \sigma\}$ are constants of electron-phonon interactions, accompanying the processes of intersubsystem Coulomb interactions. It is clear, that the second terms in (41) and in (42) describe the attraction between strongly correlated electrons, it can explain the nature of the pairing mechanism in high temperature superconductors.

The Hamiltonian $\hat{\mathcal{H}}(u)$ can be considered to be basic Hamiltonian for description of the properties of carbon NTs, produced by $\langle 100\rangle$ ion beam modification of diamond single crystals, in particular for analysis of ESR data above described. The generalization of the Hamiltonian $\hat{\mathcal{H}}(u)$ can be done by the way, proposed in [8] on the basis of hypercomplex number theory, at that it has to be taken into account, that, strongly speaking, NTs, produced by $\langle 100\rangle$ implantation cannot be described in the framework of 1D theory, since $C_4$ symmetry indicates on inequivalence of the chains along the NT axis. Let us remark, that the Hamiltonian (35) is similar to two-orbital-Hamiltonian, proposed in [27] for spectral analysis of the iron-based superconductors (SC). It will be almost coinciding in the case when $\{\alpha_1^m\} = 0$, $m = \{\pi, \sigma\}$, $\{\alpha_2^{mq}\} = 0$, $m, q = \{\pi, \sigma\}$, $J_1(j, m, q, u)$, $J_2(j, m, q, u)$ are independent on $j, m, q, u$. The difference in given case consists in inequivalence of $\sigma$ and $\pi$- subsystems, in comparison with equivalence of Fe orbitals $d_{xz}$ and $d_{yz}$, considered in [27]. However even in given more simple case the task was solved the only by numerical methods. The main result is represented in Figure 8 in [27].

The magnetic excitation spectrum carries information on the nature of magnetism and the characteristics of superconductivity. It has been discussed in the literature that an observation of a sharp quasiparticle-like resonance peak in the spin fluctuation spectrum with the onset of superconductivity may strongly indicate a sign change in the gap structure caused by the superconducting coherence factors. It has been established, that in iron pnictides a strong spin resonance occurs in the s-wave SC state. There is indication, that the spin resonance phenomenon is compatible with the $s^{\pm}$-wave SC gap. The comparison of the ESR spectra with theoretically calculated spectral function, presented in Figure 8 in [27] allows to suggest, that the spontaneous transition in ESR response in the sample studied indicates on transition to SC state, which is coexisting with antiferromagnetic (AFM) ordering. Therefore two lines - L-line and $R_b$-line - can be assigned with AFM-resonance observed in SC state. Inequivalence of the main characteristics of given lines can be attributed to strong inequivalence of two subsystems in NTs in comparison with theoretically calculated in [27]. It seems to be essential the conclusion in given work on the appearance of peak-dip-hump feature in a spectral function when the system becomes superconsonducting. We have observed two dips. It seems to be consequence of different coupling of the resonance mode to fermions in $\pi$ and $\sigma$-subsystems. Further the authors of [27] write "detailed study of the magnetic and the electronic spectrum shows that the dispersion of the magnetic resonance mode in the nearly isotropic $s^{\pm}$ superconducting state exhibits anisotropic propagating behavior in an upward pattern". Given conclusion is also in agreement with experiment. The observation of superlinear dependence in absorption kinetics is strong evidence of the mobility of spin carriers. The switching from the saturating behavior to nonsaturating behavior with superlinear absorption kinetics of $R_b$-line can be attributed to decrease of screening of static magnetic field by increase of microwave power in the range $H_1/H_1^{(0)}$ $0.75-1$. In the favour of the SC state formation indicates the unusual asymmetry extent A/B of L-line. It seems to be also understandable the increase of Q-factor by increase of deviation of A/B factor from 1. The gain of SC propagation leads to increase of of deviation of A/B factor from 1 by simultaneous losses decrease.

## IV. CONCLUSIONS

The physical origin of the mechanism of the formation of ferromagnetic ordering in carbon nanotubes produced by high energy ion beam modification of diamond single crystals in $\langle 110\rangle$ and $\langle 111\rangle$ directions has been established. It is determined by asymmetry of spin density distribution of Su-Schrieffer-Heeger topological soliton lattice formed in 1D Fermi quantum liquid state of $\pi$-electronic subsystem of given NTs. The formation in carbon NTs of antiferromagnetic ordering coexisting with superconductivity at room temperature, produced by high energy ion beam modification of diamond single crystals in $\langle 100\rangle$ direction is suggested.

[1] Erchak D.P, Penina N.M, Stelmakh V.F, Tolstykh VP, Zaitsev AM, The 7th Int.Conf.IBMM 90, Abstracts, Knoxville, USA, 1990, p.313

[2] Efimov V.G, Erchak D.P, Gelfand R.B, Penina N.M, Stelmakh V.F, VS Varichenko, Ulyashin A.G, Zaitsev AM, E-MRS 1990 Fall Meeting, Abstracts, Strasbourg, France, 1990, p.C-V/P 12

[3] K. Kawataba et al., Synth.Met. **33** (1989) 399

[4] Erchak D.P, Efimov V.G, Zaitsev AM, Stelmakh V.F, Penina N.M, Varichenko VS, Tolstykh VP, Nuclear Instrum.Meth.in Phys.Res.,B, **69** (1992) 443-451

[5] Erchak D.P, Guseva M.B, Alexandrov A.F, Alexander H, Pilar v.Pilchau A, Pis'ma v Zhurnal Experimentalnoi i Teoreticheskoi Fiziki, v.58, N 4 (1993) 268-271, JETP Letters, v.58, N 4 (1993) 275-278

[6] Ertchak D.P, Efimov V.G, Stelmakh V.F, Review, Zhurnal Prikladnoi Spectroskopii, 64, N 4 (1997) 421-449, J.Applied Spectroscopy, N 4, (1997) 433-460

[7] Ertchak D P, Efimov V G, Stelmakh V F, Martinovich V A, Alexandrov A F, Guseva M B, Penina N M, Karpovich I A, Varichenko V S, Zaitsev A M, Fahrner W R, Fink D, Physica Status Solidi, b, 203, N2, (1997) 529-548

[8] Dovlatova A, Yearchuck D, Chem.Phys.Lett., **511** (2011) 151-155

[9] Yerchuck D, Dovlatova A, J.Phys.Chem.,C, DOI: 10.1021/jp205549b

[10] , in press

[11] Yearchuck D, Yerchak Y, Alexandrov A, Phys.Lett.A, **373**, N 4 (2009) 489-495

[12] Yearchuck D, Yerchak Y, Kirilenko A, Popechits V, Doklady NANB, **52** (2008) 48-53

[13] Yearchuck D, Yerchak Y, Red'kov V, Doklady NANB, **51** (2007) 57-64

[14] Su W.P., Schrieffer J.R, and Heeger A.J, Phys.Rev.Lett., **42** 1698 (1979)

[15] Su W.P., Schrieffer J.R, and Heeger A.J, Phys.Rev.B, **22**, (1980) 2099

[16] Tomonaga S., Prog.Theor.Phys., **5** (1950) 544

[17] Luttinger J M, J.Math.Phys., **4** (1963) 1154

[18] Heeger, A.J; Kivelson, S; Schrieffer, J.R; Su, W-P *Rev.Mod.Phys.* **1988**, *60* 781-850

[19] Goldberg, I B; Crowe, H R; Newman, P R; Heeger, A.J; MacDiarmid, A G *J.Chem.Phys.* **1979**, *70*, 1132-1135

[20] Kahol, P K; Mehring, M *J.Phys.C* **1986**, *19*, 1045-1054

[21] Kuroda, S; Tokumoto, M; Kinoshita, N; Shirakawa, H *J.Phys.Soc.Jpn* **1982**, *51*, 693-694

[22] Lifshitz, E.M; Pitaevsky, L.P, Statistical Physics, part 2, M., Nauka, 1978, 448 pp

[23] Thomann H, Dalton L R, Grabowsky M, Clarke T C, Phys.Rev.B, **31**(1985) 3141

[24] Dyson, F D *Phys.Rev.* **1955**, *98*, 349-359

[25] Erchak D P, Zaitsev A M, Stel'makh V F, Tkachev V D, Phys.Tekhn.Polupr., **14**, N 1 (1980) 139 -143, Sov.Phys.Semicond., USA, **14**, N 1 (1980) 79-82

[26] Poole C P, Jr, Technique of EPR-spectroscopy, Moscow, Mir, 1970, 557 pp

[27] Zhang J, Sknepnek R and Schmalian J, Phys.Rev.B, **82** (2010) 134527